IMPACT OF ASPECT RATIO ON VOLTAGE GAIN OF QUARTZ TRAPPED-ENERGY RESONATORS

Mary E. Galanko Klemash[1], Dylan Bruno[2], Tobias M. Kiebala[2], Ryan Rudy[1], Victor Farm-Guoo Tseng[1] and Sarah S. Bedair[1]*

[1] U. S. Army Combat Capabilities Development Command – Army Research Laboratory, USA

[2] Rochester Institute of Technology, USA

ABSTRACT

This work examines the impact of electrode aspect ratio on the performance of quartz trapped-energy mode resonators in front-end wake-up receivers. In a series of resonators designed around 93 MHz with aspect ratio (AR) ranging from 1 to 2, voltage gain was directly measured at various load impedances relevant to the WUR application. Gain and quality factor (Q) are consistently maximized in devices with small resonator electrode AR, *i.e.*, approaching a width-to-length ratio of 1. This finding is in contrast with past design practices for quartz filters, where aspect ratios were chosen to minimize spurious modes in oscillators and timing applications rather than maximizing voltage gain as detailed in this work. The improved performance of devices with AR = 1 applies across a range of load impedances expected in the application as a front-end for a near-zero-power wake-up receiver.

KEYWORDS

piezoelectric devices, resonator filters, VHF resonators, wake-up receivers, Internet of Things (IoT)

INTRODUCTION

Ultra-low-power receivers are critical components of present and future Internet of Things (IoT) sensor networks. These networks are widely used to monitor distributed and inaccessible locations, such as large-scale infrastructure and agriculture. These use cases often require ultra-sensitive receivers that are available to respond to infrequent, long-range signals for months or years without battery replacement. Traditional receiver architectures cannot meet these demands for sensitivity and energy efficiency at the same time. Ultra-low-power, long-lived wake-up receivers (WURs) are one promising solution. WURs enable "near-zero" standby power consumption while remaining sensitive to a known signal. A particular modulation frequency and bit sequence triggers the WUR to briefly energize additional sensing and communication hardware. Recent work has demonstrated highly sensitive WURs over a wide frequency range, with standby power consumption as low as 10 nW [1], [2]. Key challenges include maintaining small size and high interference rejection.

Quartz piezoelectric resonators are well suited for use as a front-end in ultra-low-power WURs. The low material loss and high intrinsic quality factor (Q_m) of quartz resonators provide state-of-the-art passive voltage gain over a very narrow bandwidth [3], enabling high interference rejection in environments with crowded radio frequency (RF) spectrum usage. Quartz thickness-shear mode resonators are already a prominent commercial technology for oscillators and timing devices. These "trapped-energy" resonators typically excite a quartz membrane between opposing metal electrodes [4]. This resonator topology allows just a few critical design choices: the center frequency $\omega_r = 2\pi f_r$, which is defined to first order by the membrane thickness t; the parallel-plate shunt capacitance C_0 between the electrodes; and the electrode shape. In the common case of rectangular electrodes, the shape is defined by aspect ratio (AR) = length (L) / width (w).

Although t and C_0 are key design parameters, prior investigations have not considered the impact of electrode aspect ratio (AR = length L / width w) on the performance of quartz wake-up receiver front-ends. In prior literature on quartz trapped-energy resonators for timing applications, the typical approach to electrode geometry optimization is to suppress spurious modes [4], [5]. In general, this practice does not maximize quality factor, which in turn maximizes voltage gain and receiver sensitivity.

Based on the dominance of losses around the edge of the resonator [6], this work proposes that for a given device capacitance C_0, perimeter area should be minimized, giving AR = 1. A series of 1-port quartz resonators was fabricated with fixed f_r, fixed C_0, and AR varying between 1 and 2. Despite inter-device variation, devices with AR = 1 have the highest average voltage gain and observed quality factor Q_{gain}. This finding is broadly relevant for quartz resonators, a mature technology conducive to widespread commercial use, and for other material systems under development (e.g., [7]).

DESIGN

Resonator Design

Fig. 1 illustrates a typical quartz "trapped-energy" thickness-shear mode resonator topology. Each monolithic quartz substrate has diameter 5 mm and contains a central stepped area, or

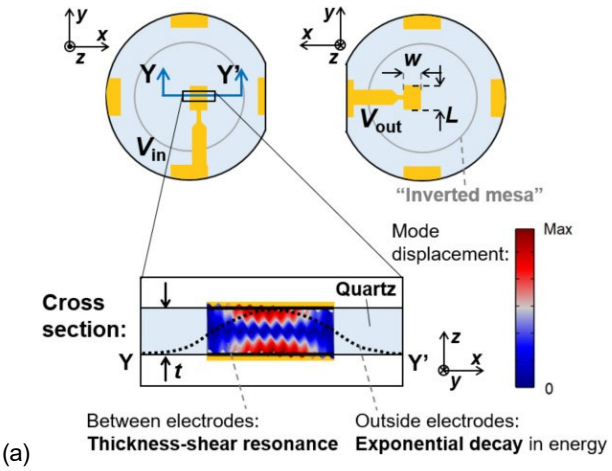

Figure 1: (a) Diagram of 1-port quartz resonator topology and thickness-shear mode shape. (b) Equivalent circuit model of quartz resonator and integrated system.

978-1-940470-04-7/HH2022/$25©2022TRF
DOI 10.31438/trf.hh2022.45

"inverted mesa," where the substrate is thinned to achieve a specific membrane thickness that defines f_r. Electrodes, traces, and pads are patterned in gold with nominal thickness around 120 nm on each side of the substrate. Rectangular electrodes with width w and length L are aligned on the top and bottom of the membrane to enclose a quartz area with thickness t and area $w \times L$. This rectangular prism-shaped section of the membrane is mass-loaded by the electrodes so that the thickness-shear mode resonance f_r of the electrode area is below the resonant frequency f_s of the surrounding membrane. Therefore, an AC voltage across the electrodes around frequency $f_r < f_s$ excites thickness-shear mode standing waves that do not propagate outside the electrode area, creating "trapped" energy in vibration modes [4]. Fig. 1(a) shows the result of a finite-element eigenfrequency simulation for the thickness-shear mode. Displacement is maximized at the membrane surface near the center of each electrode.

Fig. 1(b) shows the equivalent circuit of each thickness-shear mode resonator. C_0 arises from the parallel-plate capacitance between opposing electrodes. Other equivalent circuit values R_m, L_m, C_m are defined by f_r, C_0, and intrinsic material values for quality factor Q and electromechanical coupling factor k^2 [8]. Each trace between an electrode and a pad introduces series resistance $R_{trace} \approx 2.5\ \Omega$. In this work, the input voltage is sourced by a signal generator modeled by V_S and $Z_0 = 50\ \Omega$, in place of a WUR antenna with this equivalent circuit. The load impedance is modeled by a resistance R_L and capacitance C_L in parallel, representing the input impedance of the circuit block that loads the quartz resonator in the WUR front-end application. To measure V_{out} and ensure that it is as close as possible to the practical WUR front-end output voltage, this work uses active probes that are also modeled by input impedance $R_L \parallel C_L$ with similar values.

Minimizing Trapped Energy Loss

In prior literature on quartz trapped-energy resonators for timing applications, the most common approach to electrode geometry optimization is to maximize the separation between the fundamental frequency f_r and higher-frequency spurious modes. Shockley et al. [4] suggest doing so by ensuring that the electrode width is small enough to suppress all inharmonic overtone standing waves. Sheahan [5] refines this equation and substitutes quartz material parameters to predict a fixed optimal AR = 1.26.

This analysis does not consider energy loss from the resonator into the surrounding substrate. Shockley et al. [4] estimate that energy E decays exponentially with distance d from the electrode:

$$E = E_0 e^{-2\gamma d} \qquad (1)$$

where E_0 is proportional to the square of displacement and γ is an attenuation constant. Mindlin [6] calculates total strain energy around the resonator boundary using a surface integral over the perimeter. Assuming Equation (1) is uniform around the edge of the resonator, using this surface integral, the energy loss is approximately proportional to Equation (1) and to the resonator perimeter surface area $(2w + 2L) \times t$. Also, Q_m, a metric of energy storage relative to loss, will be higher for resonators with higher ratios of volume to surface area. Although general sources of loss in piezoelectric resonators are more complicated and are still under study [9], this work approximates that without excitation of spurious modes, the quality factor and therefore the voltage gain are maximized when $w + L$ is minimized, giving AR = 1.

Experimental Design

To specifically examine the impact of AR on performance, a series of 1-port AT-cut quartz trapped-energy resonators were fabricated within a custom commercial process (Microsemi High Performance Timing, Microchip Inc., Mount Holly Springs, PA) using the topology illustrated in Fig. 1. Each resonator had $f_r \approx 93.2$–94.2 MHz, varying AR = 1–2, and $C_0 \approx 165$ fF or $C_0 \approx 230$ fF. These two C_0 values were chosen to match the range of load capacitances expected in WUR integration while probing the impact of specific C_0 value on AR vs. gain trends. Because prior work has shown significant post-fabrication performance variation between individual resonators of a given design, this study included duplicate resonators of each design: 3 duplicates of each AR with $C_0 \approx 165$ fF, and 6 of each AR with $C_0 \approx 230$ fF.

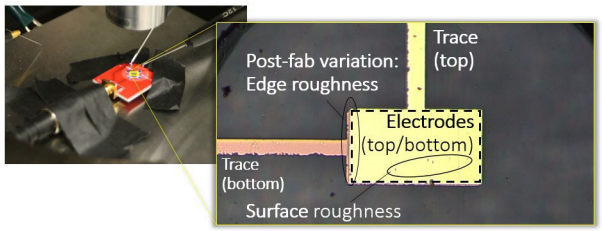

Figure 2: A typical fabricated quartz trapped-energy resonator and testbed. Traces, electrodes, and post-fabrication electrode variations are labeled.

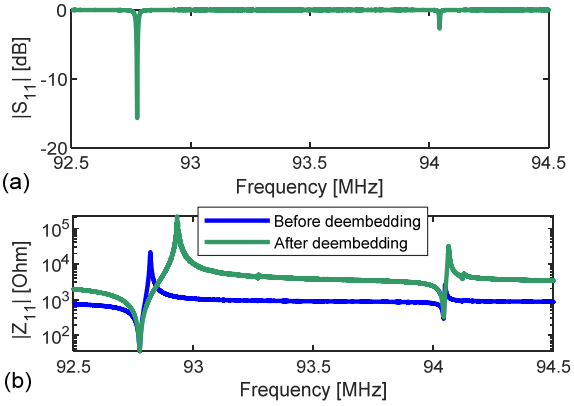

Figure 3: (a) S_{11} (de-embedded) and (b) input impedance (raw and de-embedded) versus frequency in a representative 1-port quartz resonator, measured with load $R_L \approx 0$. The closest spurious mode f_{spur} appears >10,000 ppm above the primary resonance f_r = 92.78 MHz.

RESULTS

Fig. 2 shows a typical voltage gain testbed and fabricated resonator, including electrodes with post-fabrication variation. To measure RF parameters and voltage gain, the input pad of each quartz substrate was mounted to a custom printed circuit board (PCB) on Rogers 4003 material (Rogers Corp., Chandler, AZ) using Loctite Ablestik 84-1LMI conductive silver epoxy (Henkel Electronic Materials, Irvine, CA). Input signals are routed through an SMA connector on this trace. Fig. 3 shows representative S_{11} and impedance measurements. The nearest spurious mode occurs >10,000 ppm above the primary resonance. This separation, >100× the bandwidth of either peak, is sufficient to prevent energy leakage between modes and to fit the application.

Voltage gain V_{out} / V_S is directly observed by applying $V_S = 40$ mV and landing Picoprobe high-impedance active probes (GGB Industries, Naples, FL) on the quartz output pad (V_{out}). At each load, observed quality factor $Q_{gain} = f_r / \Delta f$ is calculated by measuring the −3 dB bandwidth of V_{out}. A range of load impedances are applied by using 3 Picoprobe models that present

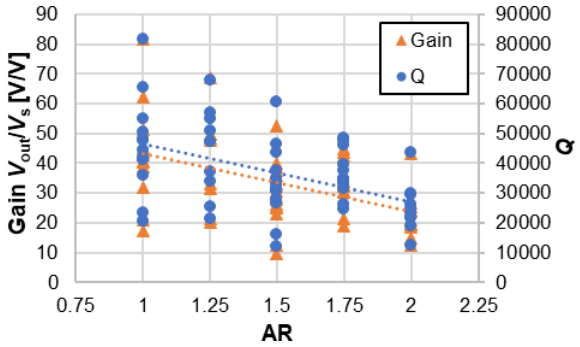

Figure 4: Voltage gain (V_{out} / V_s) and quality factor (Q), measured at load impedance R_L = 10 MΩ || C_L = 180 fF, versus aspect ratio for a series of 1-port quartz resonators with C_0 ≈ 165−230 fF.

different R_L, C_L, and by landing combinations of two probe models simultaneously such that their R_L, C_L add in parallel. The voltage gain of each device is measured several times to ensure that the result is not subject to test variations, such as probe contact quality. Typical variation between consecutive measurements is < 5%. These gain measurements were performed for each device with any C_0 and are analyzed both together and for fixed C_0 ≈ 230 fF.

All Devices

At a representative load impedance R_L = 10 MΩ || C_L = 180 fF, comparable to the input impedance of a high-performance WUR design [1], Fig. 4 illustrates trends in gain and Q_{gain} versus AR across both C_0 values. Average gain and Q_{gain} decrease proportionally with increasing aspect ratio. Although large variations in gain occur at each AR, a decrease in average gain is evident with increasing AR. Variations in gain and Q_{gain} are attributed to post-fabrication variation between resonators and are consistent with prior observations [3]. For each C_0 separately and for the complete dataset in Fig. 4, Table 1 compares the average and standard deviation in Q_{gain} for AR = 1 and AR = 2. Overall, the average Q_{gain} is about 46% higher at AR = 1 versus AR = 2. At both ARs, Q_{gain} is higher at higher C_0. This observation further suggests that lower ratios of perimeter area to electrode area enable more efficient energy trapping and less leakage.

Most notably, gain measurements in Fig. 4 show that 1-port quartz resonators can exhibit voltage gain over 80 V/V or 38 dB when loaded by a realistic WUR input impedance. This performance exceeds that of lumped-element electromagnetic component front-ends used in WURs in this frequency range [1].

Table 1: Q Measurements at Maximum and Minimum Aspect Ratio at Load R_L = 10 MΩ || C_L = 180 fF.

C_0	AR = 1		AR = 2	
	Average Q	*Standard Deviation*	*Average Q*	*Standard Deviation*
165 fF	35,100	12,300	23,300	2,500
230 fF	54,300	15,200	26,900	10,400
Any C_0	46,300	16,700	25,100	7,500

Fixed C_0

Fig. 5 examines voltage gain vs. AR exclusively for C_0 ≈ 230 fF at five high-impedance loads presented by active probes. The maximum load impedance is presented by the Picoprobe Model 19C, which has C_L ≈ 60 fF and very high R_L (>> 1 GΩ). Fig. 5(a) shows that the highest and most variable gain

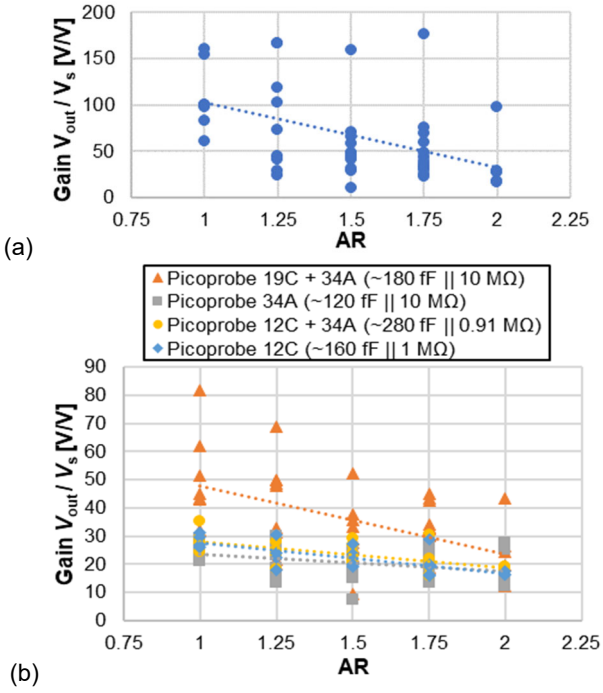

Figure 5: Voltage gain V_{out} / V_s (referenced to 50 Ω source) versus aspect ratio (AR) for a series of 1-port quartz resonators with C_0 ≈ 230 fF. (a) Gain vs. AR at maximum load impedance (~60 fF); gain is maximal and widely variable but increases at low AR. (b) Gain vs. AR at an array of realistic load impedances.

measurements occur at this load, consistent with prior observations [3]. The ultra-high-impedance probe appears to be more sensitive to contact quality and other variations between devices and between tests. Although high-impedance measurements are informative as an upper limit on voltage gain, remaining tests focus on lower load impedances, where gain measurements are less variable and are more realistic for the WUR application. For 4 load impedances with total R_L ≈ 0.9-10 MΩ and C_L ≈ 120-280 fF, Fig. 5(b) illustrates a uniform decrease in both average and maximum voltage gain with increasing aspect ratio. The average and standard deviation of voltage gain measurements are higher for certain combinations of R_L, C_L, generally higher gain for higher R_L and a particular C_L. This behavior is attributed to a known dependence of measured gain upon the electrical quality factor of the load impedance ($Q_{elec,load}$). Prior work has shown that voltage gain is limited to $Q_{elec,load}$ for the high-impedance loads of interest for wake-up receiver front-ends [10]. Loaded gain is modeled as an inverse sum of the observed open-circuit voltage gain $A_{v,OC}$ and electrical quality factor of the testbed/device materials and load:

$$A_{v,meas} \approx 1 / [\, \tan\delta_{quartz} + \tan\delta_{PCB} + 1/Q_{elec,load} + 1/A_{v,OC} \,] \qquad (2)$$

where tanδ denotes the electrical loss tangent of the quartz or PCB material. Unlike many piezoelectric resonator materials, the quartz material loss $\tan\delta_{quartz}$ < 0.0001 is so low that it may be omitted from Equation (2). The Rogers 4003 PCB material used in this work has $\tan\delta_{PCB}$ ≈ 0.002. Finally, for any load modeled by parallel resistance R_L and capacitance C_L, $Q_{elec,load}$ may be approximated as

$$Q_{elec,load} \approx \omega_r R_L C_L . \qquad (3)$$

To explore this scaling, Fig. 6 shows gain versus $1/Q_{elec,load}$. Voltage gain is measured at the same four realistic load

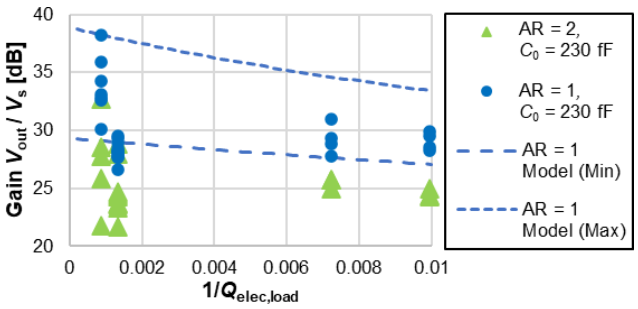

Figure 6: Voltage gain versus inverse of load electrical Q ($Q_{elec,load}$) for duplicate 1-port quartz resonators with $C_0 \approx 230$ fF and either AR = 1 or AR = 2. Dashed lines indicate model of voltage gain vs. $1/Q_{elec,load}$ are extrapolated from the highest and lowest gain measured at $1/Q_{elec,load} \approx 0.001$.

impedances examined in Fig. 5(b). Especially at the maximum $Q_{elec,load}$ applied (R_L = 10 MΩ || C_L = 180 fF), voltage gain varies significantly for a given design and load impedance but is maximized for AR = 1. Notably, at the minimum $Q_{elec,load}$ ($1/Q_{elec,load} \approx 0.01$), the average voltage gain offered by AR = 1 is higher than that of devices with AR = 2 by nearly 70%, much higher than the standard deviation of the data. These results suggest that especially in receiver circuits with lower $Q_{elec,load}$, such as those with input resistance $R_L \leq 1$ MΩ, minimizing AR is critical to maximum performance.

Gain vs. $Q_{elec,load}$ data may be compared with the Equation (2) model. Dashed lines in Fig. 6 indicate modeled $A_{v,meas}$ as modeled by extrapolating Equation (2) from the maximum and minimum voltage gain measured at the highest $Q_{elec,load}$ shown (lowest $1/Q_{elec,load} \approx 0.001$). Although most gain measurements fall between the estimates of these two functions, this envelope tends to overestimate voltage gain at lower load impedances. This discrepancy shows that improved models of gain versus $Q_{elec,load}$ and other sources of testbed loss are necessary as future work.

Future work will also examine relationships between aspect ratio, post-fabrication variation, and spurious mode placement. Additionally, similar studies of gain versus $Q_{elec,load}$ are needed in other quartz resonator designs. It is important to validate this trend at other resonant frequencies across the design range for these resonators, about 50-200 MHz. Resonators at higher frequencies may have different limitations governing resonator size versus relative spurious mode frequency. Finally, a similar study is required on gain vs. AR in 2-port quartz resonant transformers. 2-port devices are comprised of two monolithic coupled resonators, each based on the 1-port device geometry in this work. The 2-port configuration offers more design flexibility, especially in impedance matching with an antenna. In addition to varying AR, a study on 2-port resonators should vary the separation between the two coupled resonators. Although minimizing AR is still expected to minimize losses to the surrounding substrate, additional trade-offs may exist between AR, electrode separation, and yield.

CONCLUSIONS

This work shows that choosing aspect ratio (AR) = 1 maximizes voltage gain in a class of custom commercially fabricated 1-port thickness-shear mode quartz resonators. These findings broadly inform design the trapped-energy resonators to improve performance in RF sensing. Over a range of load impedances found in ultra-low-power wake-up receiver applications, resonators with AR = 1 enable voltage gain up to 80 V/V. This performance is competitive with electromagnetic transformers, but with much higher out-of-band rejection and a smaller form factor. Compared with an electromagnetic matching network around 100 MHz, which uses bulky lumped-element inductors [2], the quartz resonator has >70× smaller footprint and very low profile (<< 1 mm). While the design principles in this work apply to other resonator topologies and material systems under development, the manufacturability and low cost of quartz thickness-shear resonators provide easy, accessible prototyping and a low barrier to integration in commercial IoT.

ACKNOWLEDGEMENTS

This work was supported in part by the Army Research Laboratory under Grant W911NF-21-2-0052 and in part by the Defense Advanced Research Projects Agency (DARPA) Microsystems Technology Office (MTO). The views and conclusions contained in this document are those of the authors and should not be interpreted as representing the official policies, either expressed or implied, of the Army Research Laboratory, DARPA, or the U.S. Government. The U.S. Government is authorized to reproduce and distribute reprints for Government purposes notwithstanding any copyright notation here.

The authors wish to thank T. Daniels and D. Swarner at Microchip, Inc. for assistance with custom resonator fabrication.

REFERENCES

[1] P.-H. P. Wang, H. Jiang, L. Gao, P. Sen, Y.-H. Kim, G. M. Rebeiz, P. P. Mercier and D. A. Hall, "A 6.1-nW wake-up receiver achieving −80.5-dBm sensitivity via a passive pseudo-balun envelope detector," *IEEE Solid-state Circuits Lett.,* vol. 1, no. 5 (2018).

[2] H. Jiang, P.-H. P. Wang, L. Gao, C. Pochet, G. M. Rebeiz, D. A. Hall and P. P. Mercier, "A 22.3-nW, 4.55 cm2 temperature-robust wake-up receiver achieving a sensitivity of −69.5 dBm at 9 GHz," *IEEE J. Solid-State Circuits,* vol. 55, no. 6 (2020).

[3] M. E. Galanko Klemash, S. S. Bedair, D. A. Diamond, R. Q. Rudy, V. F.-G. Tseng, J. S. Pulskamp, and I. Kierzewski, "1-port piezoelectric resonators with >100 V/V gain," *J. MEMS*, vol. 29, no. 5 (2020).

[4] W. Shockley, D. R. Curran, D. J. Koneval, "Trapped-energy modes in quartz filter crystals," *J. Acoustical Soc. America*, vol. 41, no. 4 (1967).

[5] D. F. Sheahan, "An improved resonance equation for AT-cut quartz crystals," *Proc. IEEE*, vol. 58, no. 2 (1970).

[6] R. D. Mindlin, "High frequency vibrations of crystal plates," *Quarterly of Appl. Math*., vol. 19, no. 1 (1961).

[7] Z. Zhao, Z. Qian, and B. Wang, "Energy trapping of thickness-extensional modes in thin film bulk acoustic wave filters," *AIP Advances*, vol. 6, no. 015002 (2016).

[8] V. Kaajakari, *Practical MEMS*, Las Vegas, NV: Small Gear Publishing (2009).

[9] M. Wild, M. Bring, E. Halvorsen, L, Hoff, and K. Hjelmervik, "The challenge of distinguishing mechanical, electrical and piezoelectric losses," *J. Acoustical Soc. America*, vol. 144, no. 2128 (2018).

[10] S. S. Bedair, J. S. Pulskamp, R. Rudy, R. Polcawich, R. Cable and L. Griffin, "Boosting MEMS piezoelectric transformer figures of merit via architecture optimization," *Electron Device Letters,* vol. 39, no. 3 (2018).

CONTACT

* M. E. Galanko Klemash, tel: +1-301-394-1103; mary.e.galanko.civ@army.mil